

SLAC-PUB-2642
October 1980
(1/E)

DISCLAIMER
This document is the property of the United States Government and is loaned to you. It and its contents are not to be distributed outside your organization. It is to be used only for the purposes for which it was prepared. It is not to be used for advertising or promotional purposes, for creating new products, or for resale. It is not to be used for any other purpose without the express written permission of the United States Government. If you are not an employee of the United States Government, you are not to be used for any other purpose without the express written permission of the United States Government.

DESIGN AND PERFORMANCE OF THE NEW CATHODE

READOUT PROPORTIONAL CHAMBERS IN LASS*

G. Aiken, D. Aston, W. Dunsford, W. B. Johnson, A. Kilett,
D. W. G. S. Leith, D. McShurley, B. Ratcliff, R. Richter,
S. Suzuki, S. Shapiro, J. Va'Vra, S. H. Williams

*Stanford Linear Accelerator Center, Stanford University,
Stanford, California 94305*

L. Bird**, R. K. Carnegie, R. McKillen

Carleton University, Ottawa, Ontario, Canada K1S 5P6

T. Matsui, C. O. Pak

Nagoya University, Nagoya, Japan

ABSTRACT

The design and construction of a new proportional chamber system for the LASS spectrometer are discussed. This system consists of planar and cylindrical chambers employing anode wire and cathode strip readout techniques. The good timing characteristics of anode readout combine with the excellent spatial resolution of cathode readout to provide powerful and compact detectors. Preliminary resolution data are presented along with operating characteristics of the various devices.

Paper presented at
The 1980 IEEE Nuclear Science Symposium
November 6, 1980

* Work supported by the Department of Energy under contract No. DE-AC01-76SF00515.

* Present Address: CERN, 1211 Geneva 23 Switzerland.

** Present Address: Simon Fraser University, Burnaby, Canada.

I. INTRODUCTION

A second generation of proportional chambers has been designed, constructed and installed in the LASS spectrometer at SLAC. These new chambers replace the cylindrical and planar capacitive diode readout spark chambers previously employed in the solenoid detection system. Although these new cylindrical and planar chambers differ markedly in both geometry and construction, they do share many common features. Both employ anode wire and cathode strip readout within the same gap, the anode wires all have approximately 2 mm spacing and the half-gaps are approximately 5 mm. The anode wire readout is the same as that used in LASS for the past few years,¹ but the cathode strip readout is new and is described in a paper submitted to the 1980 Nuclear Science Symposium.²

These chambers have a readout resolving time of 150 nsec or less, which is essential for taking data in the high instantaneous data rate environment that obtains at SLAC. They have high efficiency for multiple hits, and permit the formation of match points (three dimensional space points used in track finding) in a simple unambiguous way.

This paper describes the physical characteristics of these chambers and presents their operating parameters. The algorithm employed to convert strip pulse height information to a coordinate value is discussed and preliminary results. Resolution are presented.

MASTER

EBB

II. THE PLANAR CHAMBERS

Each planar chamber has one plane of anode wires and two cathodes. The anode plane is composed of 768 vertical wires of 0.0008" diameter gold plated tungsten spaced 0.080" apart; a subset of five guard wires shapes the field at each end. Four equally spaced horizontal support wires leave a maximum unsupported length of 12.4", and sixteen polyurethane foam spacers, .25" x .25" x .20", epoxied to these support wires serve to maintain the half-gap width of 0.200".

Each cathode is formed of aluminum-mylar laminate etched to provide a pattern of 192 strips running at $\pm 45^\circ$ to the anode wires. The strips are nominally .270" wide and the strip separation is 0.050". Each of the cathodes has been surveyed after mounting on its support frame so that deformations caused by stretching can be taken into account in the coordinate reconstruction. Electrical connections are made to printed circuit cards in the frame by bending #22 AWG wire over the strips and cementing it to the aluminum with conducting epoxy. Fig. 1 is an assembly drawing of a planar chamber.

The chamber is operated with positive high voltage on the anode sense plane, while the cathode planes are at ground potential and the support wires are at approximately half the anode potential. An isolation capacitor (470 pf, at 6 kV) is used on each anode wire to protect the readout circuitry.

Each chamber has an active area approximately 61" square, and has a central region deadened by the inclusion of a mylar

plug (6.5" in diameter) epoxied to each cathode so that the high intensity beam region does not fill the central strips with data, thereby causing ambiguities and overlaps. This central region is covered by three planes of conventional 1 mm wire spacing anode readout proportional chamber, both chambers being mounted on opposite sides of a common support frame.

III. THE PROPORTIONAL CYLINDERS

Six proportional cylinders have been designed and built to surround the LASS liquid hydrogen target. The design emphasis has been to create a low mass detector for both transverse and forward-going particles, which provides large solid angle coverage, and yields dual coordinate readout from each gap. These chambers have anode wires of 0.0008" gold plated tungsten parallel to the beam axis; small angle stereo is provided by helical cathode strips at $\pm 10^\circ$ to the axis for cylinders 1-4 and $\pm 15^\circ$ for cylinders 5 and 6. A compilation of the relevant physical parameters of the cylinder and planar packages is presented in Table I.

The cylinder construction consists of a double cylinder of aluminum mylar laminate and paper honeycomb (Hexcel) resulting in a thickness of approximately 0.11 g/cm^2 . For each cylindrical detector, the inner cylinder supports the inner cathode and the anode wires, while the outer cylinder supports the outer cathode. The anode to cathode spacing is determined by Rohacell foam rings at the downstream end and G-10 rings at the upstream end. The gas seal is provided by a layer of RTV exterior to these rings. The cathodes are etched on the aluminum mylar laminate and have strip

widths as listed in Table I. The anode wire spacing is approximately 2 mm, and the cylinder active length is 100 cm for cylinders 1-4 and 87 cm for cylinders 5 and 6. The anode wires are supported at mid-length by a lucite support ring which has an insulated charge leakage wire attached and to which the anode wires are glued with Humiseal. Fig. 2 is a photograph of the cylinder package mounted to the inner surface of the upstream flux return disc of the LASS Solenoid.

IV. OPERATING CHARACTERISTICS

All of these new chambers use a magic gas mixture of 21% Isobutane, 42 Methylal, 0.75% Freon 13 B1 and the balance Argon. Fig. 3 shows a representative plateau curve of efficiency versus high voltage for a planar chamber in use at LASS. Since each chamber must be operated at that voltage for which the cathode readout is efficient, the anode cluster size must be limited by adjusting the threshold of the anode readout. The plateau curve presented for the anode readout is one for which the threshold for pulse detection was set at 220 pV (0.12 V on the reference voltage) rather than at 300 pV which has been the nominal operating point for the conventional proportional chambers in the LASS system. The spatial resolution (σ) of the anode coordinate measurement for chambers having 2 mm wire spacing has been measured to be approximately 0.6 mm. Fig. 4 shows a typical variation of pulse height with high voltage for the central cathode strip of a cluster

V. DISCUSSION OF PULSE HEIGHT DATA

The objective in building chambers of the type discussed above is to be able to use a series of pulse heights on adjacent broad

cathode strips for the precise determination of a coordinate somewhere on one of the strips. For such a series of adjacent strips, that strip which has the highest pulse height may be readily determined. The assumption is then made that the true coordinate lies somewhere within this central strip. For the strips on either side of the central strip, the ratio of the pulse height to that of the central strip may be calculated and a scatter plot of one ratio against the other generated. Independently of any assumption concerning the relationship of pulse height to position there must exist a unique locus of points on this plot if we are to succeed in generating an algorithm relating pulse height information to position. In Fig. 5 such a scatter plot is shown for data from one of the planar PWC's.

Many authors have attempted to describe the positive charge distribution on a PWC cathode caused by an avalanche at the anode³⁻⁸. These studies have been made primarily with test arrangements placed in well defined hadron beams or have used X-ray sources. The spatial resolution (σ) obtained varies from 86 - 150 μm in the case of particle beams to approximately 35 μm for the X-ray source. The results achieved seem to be independent of readout electronics, but vary significantly with gas composition, gas gain, time gate, and chamber parameters like gap size, wire spacing, and strip dimension. In reference 7, the optimum geometry for the best spatial resolution is discussed and the recommendation made that the cathode strip width and the half-gap be approximately equal. In most of these analyses a centroid method has been used for

extracts the information from the central region of the

In contrast, the data presented in Fig. 5 are obtained from large chambers. In seeking a more satisfactory balance had to be struck between the advantages of spatial resolution and contrast, and the cost of the system. To this end, a strip width larger than the half-gap is used. Furthermore, the studies to be discussed below indicate that the center method is not the most effective for the present system.

Consider a center charge between two parallel, infinite, conducting planes. The charge results in a field in the conducting plane of $E = \sigma/\epsilon_0$ and an infinite line of image charges. The solution to this idealized problem results in the field distribution in Fig. 6 for the geometry of the planar chamber central strip with $h = 0.127$ cm, $g = 0.127$ cm, and $l = 0.127$ cm. Qualitative comparisons of the data presented in Fig. 5 are found to be very sensitive to the geometry of the chamber. For example, the dashed curve, (b), of Fig. 5 represents data for the strip width being equal to the half-gap ($h = g = 0.127$ cm). It is found that the intense band of Fig. 5 is well-represented by the shaded region, (c), of Fig. 6; the upper and lower boundaries of this region correspond to solutions of the idealized problem for a strip width of 0.320 cm and half-gap values of 0.190 cm and 0.1 cm, respectively.

The solution to the idealized problem yields a relationship between pulse height ratio and position within the central strip; a

the validity of this assumption. In a multitrack high magnetic field environment such as the LASS spectrometer where a typical event may have six or more charged tracks, the ideal coordinate measuring device is one in which all coordinates are measured at the same position along the beam (z). For the existing single readout chambers, the z separation of the coordinate planes typically results in the creation of two to three times as many space points as are real. With the new, dual readout chambers, the fact that the three coordinates are in effect measured at the same z greatly reduces this problem. This has a direct impact on the accuracy and speed of the track finding programs.

Fig. 10 shows typical pulse height distributions for a planar chamber operated at 3500V. Fig. 10(a), (b) is the distribution of pulse height for the central strip and Fig. 10(c) that for the larger of the pulse heights on the adjacent strips. It should be noted that in Fig. 10(a) only about 1% of the data fall in the overflow bin. Avalanches which are so large as to saturate the pulse height for the central strip can still be used to generate coordinate values. An algorithm can be generated which uses only the left and right-hand strips to predict the coordinate values, since the technique discussed above requires only two strips rather than the three or more needed for the centroid method.

In Fig. 10(b) the most probable peak pulse height occurs approximately at channel 450. This corresponds to a charge of about 15 pC at the SHAM input and is equivalent to a charge of approximately 400×10^{-15} coulomb collected by the electronics on that cathode strip.

Fig. 11 shows the sum of the pulse heights on one cathode compared with that on the other cathode when anode corroboration is required. It is expected that the width of the diagonal band will be significantly reduced when channel to channel pulse height calibration corrections are incorporated. The linearity of the plot implies that the number of trial combinations of coordinates in situations where more than one particle passes through the chamber may be reduced by comparing pulse height sums and pairing cathode coordinates of similar total charge. This additional information should then further reduce the number of spurious space points generated. It is amusing to note here, that this is one of the few instances where Landau fluctuations are of some benefit. This feature is demonstrated in Fig. 12. Two particles having passed through the chamber yield two cathode coordinates each. Anode corroboration selects the correct pairings and it can be seen that the correct pairings are those which have similar total charge.

It should be emphasized that the data presented in this paper are preliminary in nature. Channel to channel pulse height corrections have not yet been incorporated, and, in particular, pedestal subtractions have not yet been done on an individual channel basis. The necessity for applying quadratic corrections to the gain has also not yet been investigated. In addition, studies are still under way to select the optimum operating voltage for the individual chambers.

Preliminary results for the cylindrical chambers are similar to those presented above.

VI. SUMMARY AND CONCLUSIONS

A second generation of proportional chambers has been developed for use in the LASS spectrometer at SLAC. These chambers employ both anode and cathode strip readout within the same gap, and yield a resolving time for both the anode and cathode readout which is less than 150 nsec. The spatial resolution is good (34,300 μ m), and is obtained by utilizing a new algorithm for conversion of pulse height data to coordinate value. Three dimensional space points are determined from coordinate information generated by a single gap, thus greatly simplifying the problem of pattern recognition for charged particle tracks in an intense magnetic field. It has also been shown that the problem of handling multiple hits may be greatly simplified by pairing coordinates having approximately equal total charge on each cathode foil.

The observed spatial resolution has verified the stability of the readout electronics which has been crucial to the above studies. In addition, it has been shown that good spatial resolution can be obtained with strip widths substantially larger than the half-gap, thereby resulting in a significant saving in readout electronics costs.

VII. ACKNOWLEDGEMENTS

The authors would like to thank Bill Walsh, Frank Holst and Annette Nicholson for their help in assembling the system. We would also like to thank Herman Zais and his entire organization at SLAC for their help in constructing the planar proportional

chambers; in particular, special thanks are due Hardy Bowden and Bill Fleet who labored many long months on them. At Carleton University special thanks are extended to Louis Raffler, Barbara Ellspermann and Larry Sainsbury for their fine efforts in building and testing the cylindrical package.

REFERENCES

1. A Proportional Chamber Front End Amplifier and Pulse Shaping Circuit, S. L. Shapiro, M. G. D. Gilchrist and D. C. McShurley, SLAC-PUB-1713, February 1976; IEEE Trans. Nucl. Sci. NS23 (1976) No. 1, pp. 269.
2. A Deadtimeless Shift Register Style Readout Scheme for Multiwire Proportional Chambers, S. L. Shapiro, M. G. D. Gilchrist, R. G. Friday, SLAC-PUB-1714, February 1976; IEEE Trans. Nucl. Sci. NS23 No. 1 269-273.
3. A low Noise PWC Cathode Readout System, F. Cisneros, D. Hutchinson, D. McShurley, R. Richter, S. Shapiro. Presented to the 1980 IEEE Nucl. Sci. Symposium; SLAC-PUB-1767, Oct. 1980.
4. G. Fischer and J. Pich NIM 100 (1972) 515-521
5. G. Charpak, F. Sauli; NIM 110 (1973) 481-485
6. A. Broskin, G. Charpak, C. Denterre, J. Matewski, A. Pellegrino, F. Sauli, and J. C. Santlard; NIM 153 (1977) 29-39.
7. G. Charpak, G. Peterson, A. Pellegrino and F. Sauli; NIM 148 (1978) 471-482.
8. F. Satti, A. Longoni, B. Okano, E. Senenza; NIM 163 (1979) 84-92.
9. A Position Sensitive Parallel Plate Avalanche Counter to Detect Minimum Ionizing Particles, M. Urban, W. R. Groves, C. Bell. Presented at the International Conference on Experimentation at LEP, Uppsala, Sweden June 16-20, 1980. Submitted to NIM.

FIGURE CAPTIONS

1. Assembly drawing of a planar proportional chamber.
2. Photograph of the cylinder package mounted to the inner surface of the upstream flux return disc of the LASS Solenoid.
3. A representative plateau curve for a planar PWC.
4. A representative curve showing pulse height variation versus high voltage for a planar PWC.
5. Scatter plot showing the left/center pulse height ratio plotted against the right/center ratio.
6. The locus of points for the solution to the idealized problem for:
 - a) planar chamber geometry anode-cathode gap of .200"; conducting strip of 0.270"; insulating gap of 0.050".
 - b) anode-cathode gap of .200"; conducting strip of 0.150"; insulating strip of 0.050".
 - c) planar chamber geometry with anode-cathode gap set equal to 0.150" and 0.190" for the lower and upper curves respectively.
7. Plot of pulse height ratio versus position within the central strip.
8. a) The difference between the coordinate generated from the two cathodes and the actual anode position prior to correcting the cathode data for mechanical distortion of the cathode tails.
b) The same plot after correcting for mechanical distortions.
9. a) A map of the anode plane made by using cathode coordinates in the vicinity of the deadened central region.
b) The same plot on a finer scale after displacing the chamber horizontally by 8" to allow the incident beam to strike the active regions.

10. a) The distribution of pulse height for the central strip of a cluster from a planar chamber. (50 counts/bin)
 - b) The distribution of Fig. 10(a) on a finer scale. (10 counts/bin)
 - c) The distribution of the larger of the adjacent strip pulse heights. (10 counts/bin)
11. Scatter plot showing the relationship between the summed pulse height on one cathode and that on the other cathode when anode corroboration is required.
 12. An illustration of the feature that the correct pairing of the cathode coordinates, as confirmed by anode corroboration, correlates clusters of similar total charge.

TABLE

| Cylinder Number | Apode Radius (in) | Number of Wires | Wire Diameter (mm) | Apode Circumference (mm) | Number of Wires in Apode Circumference | Number of Wires in Apode Circumference | Wire Angle |
|-----------------|-------------------|-----------------|--------------------|--------------------------|--|--|------------|
| 1 | 7.347 | 100 | 0.10 | 45.77 | 457 | 42 | 10° |
| 2 | 9.369 | 100 | 0.10 | 59.15 | 591 | 56 | 10° |
| 3 | 12.987 | 100 | 0.10 | 80.91 | 809 | 76 | 10° |
| 4 | 16.552 | 100 | 0.10 | 103.81 | 1038 | 96 | 10° |
| 5 | 20.41 | 100** | 0.10 | 127.67 | 1276 | 122 | 15° |
| 6 | 26.62 | 100** | 0.10 | 166.67 | 1667 | 161 | 15° |
| Planar Chamber | - | 100 | 0.10 | 150.80 | 1508 | 142 | 45° |

* Pit R is defined as a circle, perpendicular to the axis.

** R is the apode radius, but wires are read out together as one coordinate. Adjacent wires are connected together at the chamber, then near the ampifiers adjacent wires are again grouped together on a pedestal.

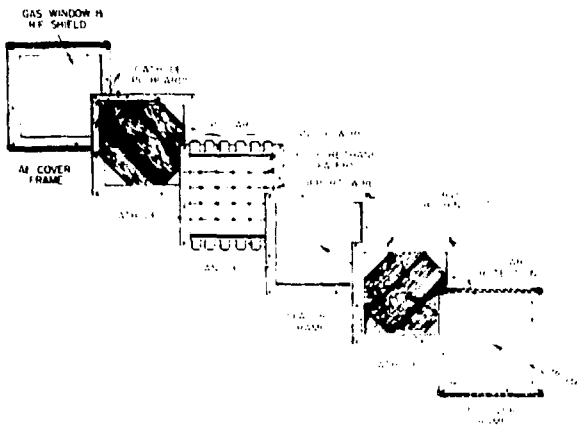


Fig. 1

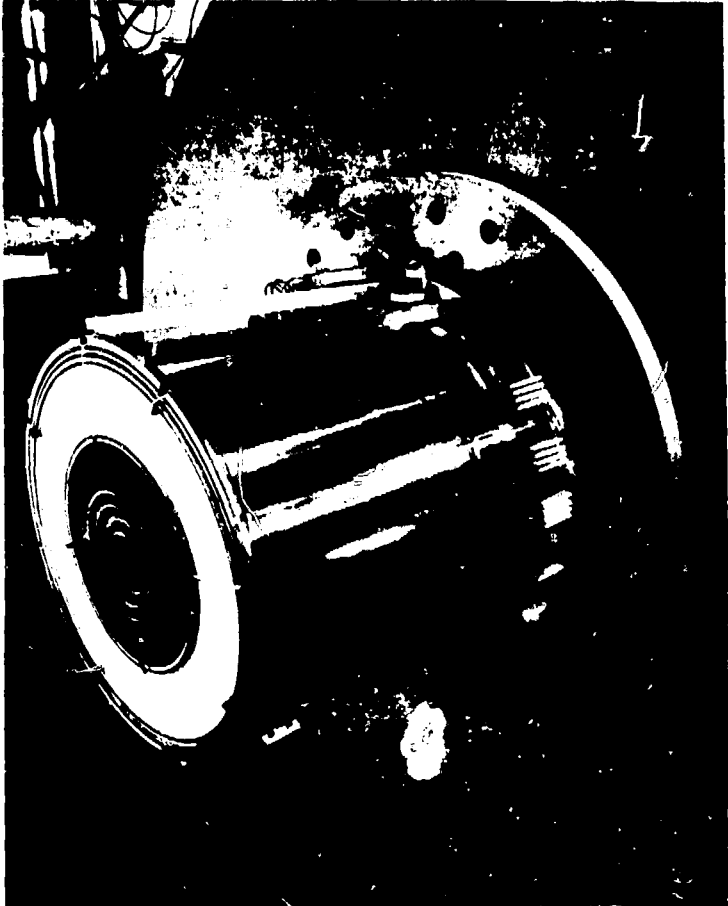


Fig. 2

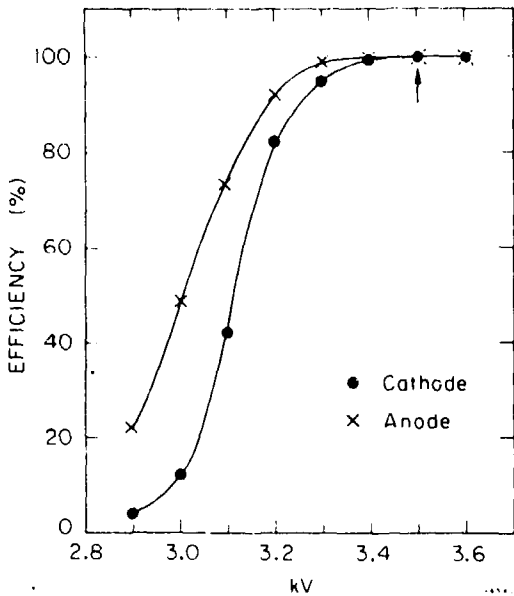


Fig. 3

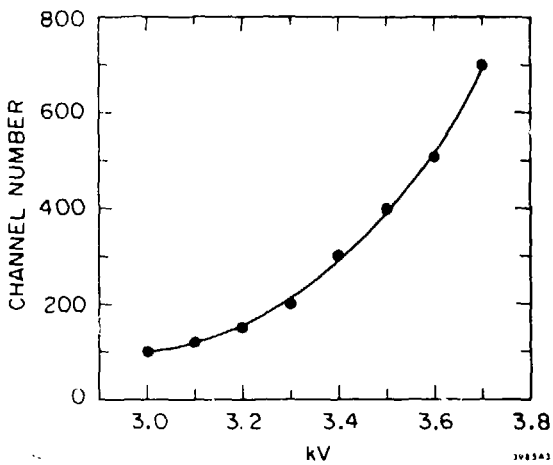


Fig. 4

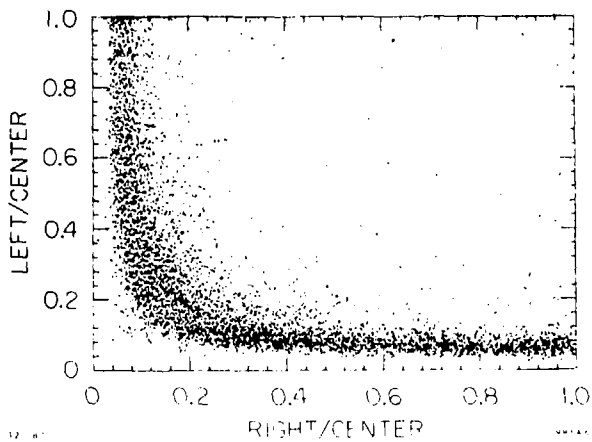


Fig. 5

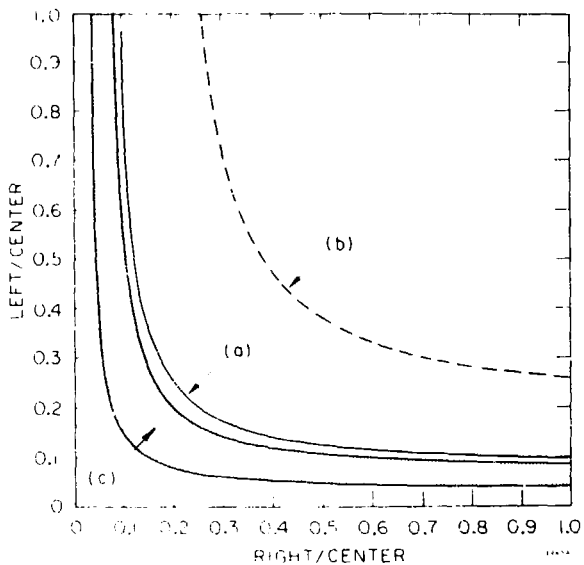


Fig. 6

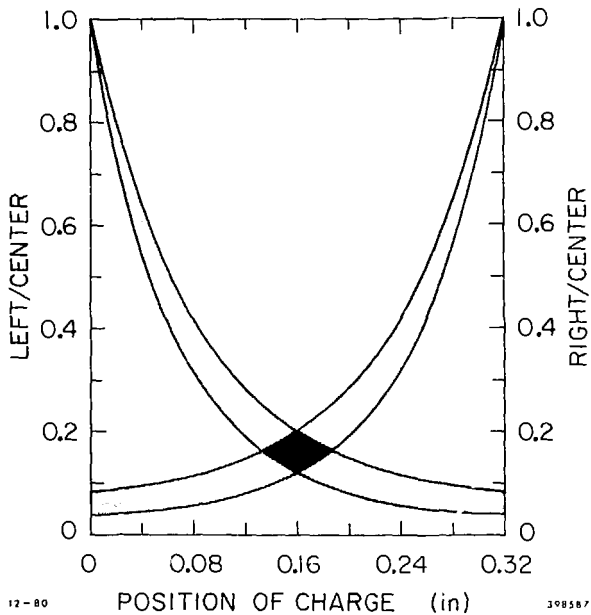


Fig. 7

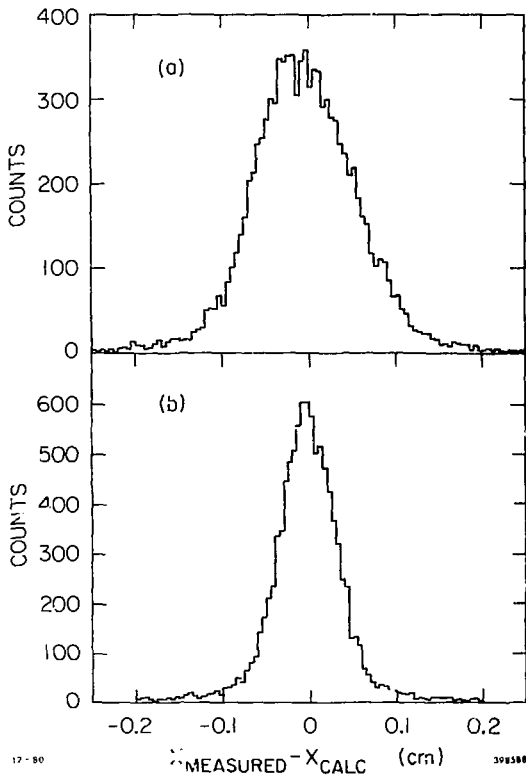


Fig. 8

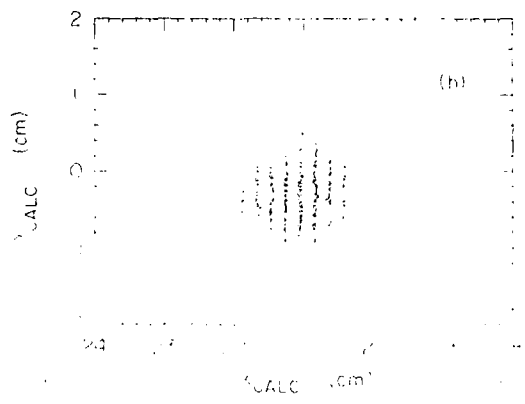
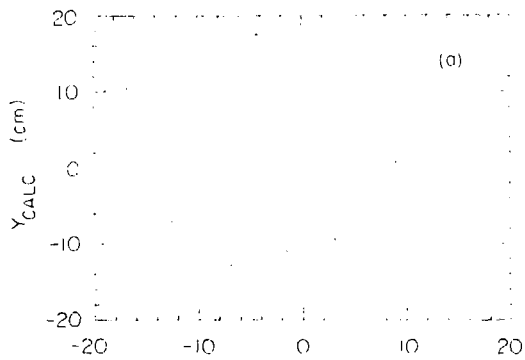


Fig. 9

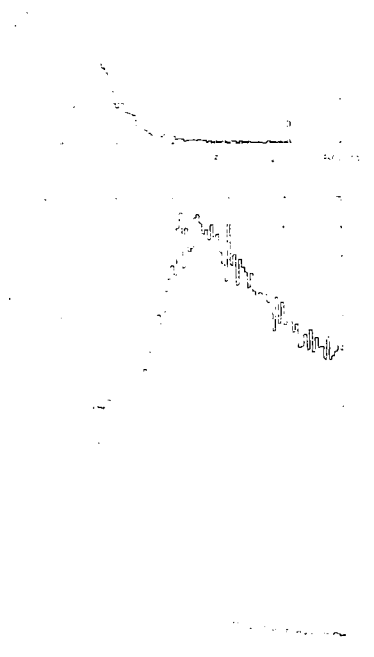


Fig 10

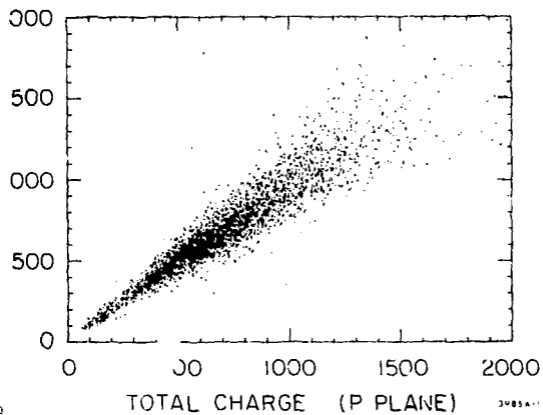
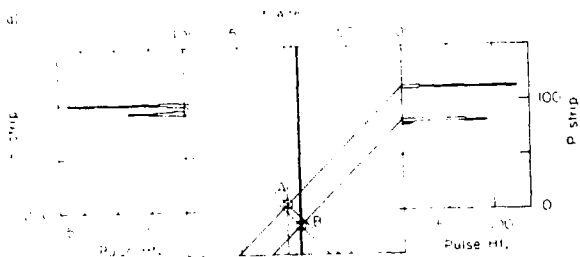


Fig. 11



(b)



Fig. 12